

Cannabinoid receptor type 2 is time-dependently expressed during skin wound healing in mice

Ji-Long Zheng · Tian-Shui Yu · Xiao-Na Li ·
Yan-Yan Fan · Wen-Xiang Ma · Yu Du · Rui Zhao ·
Da-Wei Guan

Received: 23 February 2012 / Accepted: 3 July 2012 / Published online: 20 July 2012
© Springer-Verlag 2012

Abstract Dynamic localization of CB2R and quantitative analysis of CB2R mRNA during skin wound healing in mice were performed. Co-localization of CB2R with F4/80 or α -SMA was detected by double-color immunofluorescence microscopy. A total of 110 male mice were divided into control, injury, and postmortem groups. Sixty-five mice were sacrificed, followed by sampling at 0.5 h–21 days post-injury. Five mice without incision were used as control. The other 40 mice that received incised wound were sacrificed at 5 days after injury. The samples were collected at 0 h–3 days postmortem. In the uninjured controls, CB2R immunoreactivity was

detected in the epidermis, hair follicles, sebaceous glands, dermomuscular layer, and vascular smooth muscle. In the incision groups, polymorphonuclear cells, macrophages, and myofibroblasts showed positive staining for CB2R. Morphometrically, the average ratios of CB2R-positive cells were more than 50 % at 5 days post-wounding, whereas it was <50 % at the other posttraumatic intervals. The average ratios of CB2R-positive macrophages maximized at 3 days post-wounding, and the average ratios of CB2R-positive myofibroblasts peaked at 5 days post-wounding. The relative quantity of CB2R mRNA expression maximized at posttraumatic 5 days in comparison with control as detected by real-time PCR, with an average ratio of >4.10, which was also confirmed by Western blotting. There was no significant change for CB2R protein within 6 h postmortem and for mRNA within 3 h postmortem as compared with the control group. In conclusion, dynamic distribution and expression of CB2R suggest that CB2R is involved in modulating macrophages and myofibroblasts in response to inflammatory event and repair process in mouse skin wound healing, and CB2R is available as a marker for wound age determination.

Electronic supplementary material The online version of this article (doi:10.1007/s00414-012-0741-3) contains supplementary material, which is available to authorized users.

J.-L. Zheng · T.-S. Yu · Y.-Y. Fan · W.-X. Ma · R. Zhao ·
D.-W. Guan (✉)
Department of Forensic Pathology,
China Medical University School of Forensic Medicine,
No.92, Beier Road, Heping District,
Shenyang, Liaoning Province 110001, People's Republic of China
e-mail: dwguan@mail.cmu.edu.cn

D.-W. Guan
e-mail: dwguan007@yahoo.com.cn

J.-L. Zheng · Y. Du
Department of Forensic Medicine,
China Criminal Police University,
No.83, Tawan Road, Huanggu District,
Shenyang, Liaoning Province 110035, People's Republic of China

T.-S. Yu
Key Laboratory of Evidence Science, China University of Political
Science and Law, Ministry of Education,
Beijing 100040, People's Republic of China

X.-N. Li
Department of Chemistry,
China Medical University School of Basic Medicine,
No.92, Beier Road, Heping District,
Shenyang, Liaoning Province 110001, People's Republic of China

Keywords Wound age determination · Skin incision ·
CB2R · Macrophage · Myofibroblast · Real-time PCR

Introduction

It is generally acknowledged that the endogenous cannabinoid system is ubiquitous in human and rodent. There is increasing evidence that this system plays an important role in a wide variety of physiopathological processes. The endogenous cannabinoid system is composed of the cannabinoid receptor type 1 and 2 (CB1R and CB2R), the endogenous ligands (endocannabinoids), and enzymes that synthesize and degrade endocannabinoids. As first described by Munro et al., CB2R is identified in macrophages in the marginal zone of the spleen

[1]. It is currently accepted that CB2R is mainly expressed in immune cells including neutrophils, eosinophils, monocytes, natural killer cells, mast cells, dendritic cells, and subtypes of B and T cells in vitro [2–9]. A recent study has demonstrated the presence of cannabinoid receptors in the human skin. CB2 immunoreactivity is observed in cutaneous nerve fiber bundles, mast cells, macrophages, epidermal keratinocytes, and the epithelial cells of hair follicles, sebaceous glands, and exocrine sweat glands [10]. Although the physiological roles of CB2R have not yet been elucidated during skin wound healing, recent researches have shown that CB2R is closely involved in inflammatory response and fibrotic repair of tissue injury. In an animal model for cutaneous contact hypersensitivity, mice lacking both CB1R and CB2R or wild-type mice with intraperitoneal administration of the CB2R antagonist SR144528 exacerbate allergic inflammation [11]. However, acute oral or topical administration of the CB2R antagonist SR144528 appears to ameliorate skin inflammatory responses [12, 13], indicating that CB2R antagonism may be initially beneficial but adverse upon chronic blockade. Besides, CB2^{-/-} mice are more sensitive to bleomycin-induced dermal fibrosis than CB2^{+/+} mice, and show increased dermal thickness. Increased dermal fibrosis is also observed upon treatment with CB2R antagonist AM630. In contrast, selective CB2R agonist JWH-133 reduces leukocyte infiltration and dermal thickening [14]. Based on the studies mentioned above, a tenable hypothesis is that CB2R may participate in inflammatory and fibrous repair process after skin incision.

In the present study, we have immunohistochemically investigated dynamic distribution of CB2R during skin wound healing, with special consideration on the immunolocalization of CB2R in macrophages and myofibroblasts. Moreover, time-dependent expression of CB2R was examined by Western blotting and real-time PCR for its practical applicability as a parameter to wound age determination.

Materials and methods

Animal model of skin wound

Establishment of an animal model of incised skin wound was described previously [15]. Briefly, a total of 110 male adult healthy BALB/c mice, each weighing 35–40 g, were divided into control, injury, and postmortem groups. Of the 110 mice, 65 were anesthetized by intraperitoneal injection with sodium pentobarbital. Subsequently, a 1.5-cm-long incision was made with a scalpel in the skin layer on the central dorsum under sterile technique. After incision was made, each mouse was individually housed in a cage and fed with commercial mouse chow and distilled water to prevent bacterial infection. All mice were kept under a 12-h light–dark cycle with specific pathogen-free conditions during the

experiments. After the animals were sacrificed by cervical dislocation after anaesthetization, 1.5 × 1-cm specimens were taken from wounded sites at 0.5 h, 1 h, 3 h, 6 h, 12 h, 1 day, 3 days, 5 days, 7 days, 10 days, 14 days, 17 days, and 21 days post-injury (five mice at each posttraumatic interval). One half of the specimen was used for immunohistochemical procedures, and another was used for Western blotting and real-time PCR. Five mice without incision were used as control.

To investigate the influence of postmortem RNA degradation on detection of CB2R mRNA, 40 mice were sacrificed at 5 days post-injury, and the carcasses were kept under a conditioned environment with ambient temperature of 20–22 °C and humidity of 70–75 %. The wounded skin samples were collected at 0 h, 0.5 h, 1 h, 3 h, 6 h, 12 h, 1 day, and 3 days after death (five mice at each postmortem interval).

Experiments conformed to the “Principles of Laboratory Animal Care” (National Institutes of Health published no. 85–23, revised 1985) that sought to minimize both the number of animals used and any suffering that they might experience, and were performed according to the Guidelines for the Care and Use of Laboratory Animals of China Medical University.

Tissue preparation and immunohistochemical staining

The skin specimens were immediately fixed in 4 % paraformaldehyde in phosphate-buffered saline (PBS; pH 7.4) and embedded in paraffin. Five-micrometer-thick sections were prepared. Immunostaining was performed using the streptavidin–peroxidase method. Briefly, tissue sections were mounted on the APES-coated glass slides. The sections were deparaffinized in xylene, rehydrated with a series of graded alcohol, and then heated in 0.01 mol/L sodium citrate buffer (pH 6.0) with a medical microwave oven for antigen retrieval. Subsequently, hydrogen peroxide (3 %) was applied for quenching endogenous peroxidase activity. The sections were blocked with 10 % nonimmune goat serum to reduce nonspecific binding. Then, tissue sections were incubated with rabbit anti-CB2 polyclonal antibody (dilution 1:400; sc-25494, Santa Cruz Biotechnology, CA, USA) overnight at 4 °C, followed by incubation with Histostain-Plus Kit according to the manufacturer's instructions (Zymed Laboratories, South San Francisco, CA, USA). The sections were routinely counterstained with hematoxylin. As immunohistochemical controls for immunostaining procedures, some sections were incubated with normal rabbit IgG or PBS in place of the primary antibody. Hematoxylin–eosin staining was conventionally conducted. For morphometric analysis, polymorphonuclear cells (PMNs), mononuclear cells (MNCs), and fibroblastic cells (FBCs) in the peripheral zone of the wound and wound

cavity were evaluated. In each section, ten microscopic fields at 400-fold magnification were randomly selected, and the ratio of CB2R-positive cells to the total number of cells was calculated in each microscopic field. The average ratio of the ten selected microscopic fields was evaluated in each wound specimen and expressed as percentage.

Double indirect immunofluorescence

For identification of macrophages, co-localization of CB2R and F4/80 (macrophage marker) was conducted by double direct immunofluorescence method. Briefly, sections were blocked with 5 % bovine serum albumin (BSA) and incubated with rabbit anti-CB2R polyclonal antibody (dilution 1:50; sc-25494, Santa Cruz Biotechnology, CA, USA) and rat anti-F4/80 monoclonal antibody (dilution 1:50; sc-52664, Santa Cruz Biotechnology, CA, USA) overnight at 4 °C. Then, the sections were incubated with Rhodamine (TRITC)-AffiniPure Goat anti-Rabbit IgG (dilution 1:100; 111-025-045, Jackson ImmunoResearch, PA, USA) and Alexa Fluor® 488 donkey anti-rat IgG (dilution 1:100; A21202, Invitrogen, CA, USA) at room temperature for 2 h. Nuclei were counterstained with Hoechst 33258. Normal rabbit or rat IgG or PBS was used to replace the primary antibodies as negative control.

For identification of myofibroblasts, co-localization of CB2R and α -smooth muscle actin (α -SMA) was conducted by double indirect immunofluorescence method. The sections were blocked with 10 % nonimmune goat serum to reduce nonspecific binding. Then, tissue sections were incubated with rabbit anti-CB2R polyclonal antibody (dilution 1:50; sc-25494, Santa Cruz Biotechnology, CA, USA) at room temperature for 2 h. The sections were further incubated with biotinylated donkey anti-rabbit IgG (dilution 1:150; ab6801, Abcam, Cambridge, UK) and streptavidin, Alexa Fluor® 555 conjugate (dilution 1:200; S-21381, Invitrogen, CA, USA). Then, tissue sections were incubated with rabbit anti- α -SMA polyclonal antibody (dilution 1:50; ab5694, Abcam, Cambridge, UK) overnight at 4 °C after blocked with 5 % BSA. After incubation with FITC-AffiniPure Goat anti-Rabbit IgG (dilution 1:100; 111-095-045, Jackson ImmunoResearch, PA, USA) at room temperature for 2 h, the nuclei were counterstained with Hoechst 33258. Normal rabbit IgG or PBS was used instead of primary antibody as negative control. The sections were observed under a fluorescence microscope with Digital CCD Imaging System.

For positive cell ratio evaluation, in each section, ten microscopic fields at 400-fold magnification were randomly selected in the peripheral zone of the wound and wound cavity, and the ratio of CB2R-positive cells to the total number of cells in each positive cell type was calculated in each microscopic field. The average ratio of the ten selected

microscopic fields was evaluated in each wound specimen and expressed as percentage.

Protein preparation and immunoblotting assay

The skin samples were diced into very small pieces using a clean razor blade and homogenized with a sonicator in RIPA buffer (sc-24948, Santa Cruz Biotechnology, CA, USA) containing protease inhibitors at 4 °C. Homogenates were centrifuged at 12,000 \times g for 30 min at 4 °C three times, and the resulting supernatants were collected. The protein concentrations were determined by BCA method. Aliquots of the supernatants were diluted in an equal volume of 5 \times electrophoresis sample buffer and boiled for 5 min. Protein lysates (50 μ g) were separated on a 12 % sodium dodecyl sulfate–polyacrylamide electrophoresis gel and transferred onto polyvinylidene fluoride membranes (Millipore, Billerica, MA, USA). After being blocked with 5 % nonfat dry milk in Tris-buffered saline–Tween#20 at room temperature for 2 h, the membranes were incubated with rabbit anti-CB2R polyclonal antibody (dilution 1:400; sc-25494, Santa Cruz Biotechnology, CA, USA) at 4 °C overnight and horseradish peroxidase conjugated goat anti-rabbit IgG (sc-2004, Santa Cruz Biotechnology, CA, USA) at 1:6,000 dilution at room temperature for 2 h. The blotting was visualized with Western blotting luminol reagent (sc-2048, Santa Cruz Biotechnology, CA, USA) by Electrophoresis Gel Imaging Analysis System (MF-ChemiBIS 3.2, DNR Bio-Imaging Systems, ISR). Subsequently, Western blotting data were semiquantitatively analyzed using Scion Image Software (Scion Corporation, MD, USA). The relative protein levels were calculated by comparison with the amount of GAPDH (# G13-61M, SignalChem, Canada) as a loading control.

Real-time PCR

Total RNA was isolated from the skin specimens (weight, 100 mg) by use of RNAiso Plus (9108, Takara Biotechnology, Shiga, Japan) according to the manufacturer's instructions. The RNA pellet was air-dried for 5 min and resuspended in 30 μ l diethylpyrocarbonate-treated dH₂O. OD values for each RNA sample were measured by ultraviolet spectrophotometer. A260/A280 ranged from 1.8 to 2.0. Using 1 μ g of total RNA, 28S, 18S, and 5.8S (5S) rRNA were observed clearly by agarose gel electrophoresis. The RNA was reversely transcribed into cDNA using PrimeScript™ RT reagent Kit (RR037A, Takara Biotechnology). cDNA synthesis was performed in a 20- μ l reaction mixture containing 11 μ l RNase-free dH₂O, 4 μ l 5 \times Prime Buffer, 1 μ l Oligo dT, 1 μ l Random 6 mers, 1 μ l RT Enzyme Mix I, and 1 μ g of total RNA. The resulting cDNA was used for real-time PCR with the sequence-specific primer pairs for

CB2R and β -actin (Table 1). PCR amplification used SYBR[®] PrimeScript[™] RT-PCR Kit (RR081A, Takara Biotechnology). Aliquots of 20 μ l reaction mixture contained 6.8 μ l dH₂O, 10 μ l SYBR[®] Premix Ex Taq[™] (2 \times), 0.4 μ l PCR Forward Primer (10 μ M), 0.4 μ l PCR Reverse Primer (10 μ M), 0.4 μ l ROX Reference Dye II (50 \times) *3, and 2 μ l cDNA. Amplification was performed by one round of initial denaturation at 95 °C for 30 s, step-cycle mode of 40 rounds of denaturation at 95 °C for 5 s, annealing and extension at 60 °C for 34 s by Applied Biosystems 7500 real-time PCR System using 96-well optical reaction plate. To exclude any potential contamination, negative controls were also performed with dH₂O instead of cDNA during each run. No amplification product was detected. The real-time PCR procedure was repeated at least three times for each sample.

Statistical analysis

Data were expressed as means \pm standard deviation (SD) and analyzed using SPSS for Windows 11.0. The one-way ANOVA was used for data analysis between two groups. Difference associated with $P < 0.05$ was considered statistically significant.

Results

Immunohistochemical staining and co-localization of CB2R with F4/80 and α -SMA

In the uninjured skin specimens, positive staining of CB2R was detected in the epidermis, hair follicle, sebaceous glands, cutaneous muscle layer, and vascular smooth muscle cell. In the injured skin samples, a few PMNs showed CB2R-positive reaction from 1 to 12 h. At 1 and 3 days, CB2R positive staining was observed mostly in round-shaped MNCs. From 5 days post-wounding onward, CB2R immunoreactivity was mainly detected in FBCs. At

14 days after injury, there were still a few MNCs and a substantial proportion of FBCs labeled with CB2R antibody. At 21 days after injury, a small number of FBCs showed to be CB2R positive. No false positive staining was detected in the sections used as immunohistochemical controls (Fig. 1a–f). Morphometrically, there is no significant differences in the average ratio of CB2R-positive cells between posttraumatic 0.5, 1, 3 h and control, or 17, 21 days and control ($P > 0.05$). The average ratios of CB2R-positive cells to total cells were peaked with over 50 % at 5 days post-wounding, whereas it was < 50 % at the other posttraumatic intervals ($P < 0.05$, Supplemental Fig. 1).

In the control group, a few CB2R⁺/F4/80⁺ cells were observed in the dermal layer of normal skin, indicating that resident tissue macrophages were CB2R-positive as detected by double direct immunofluorescence staining. The CB2R⁺/F4/80⁺ cells started to accumulate at 1 day after injury (Fig. 2) and maximized in number at 3 days after injury. Thereafter, CB2R⁺/F4/80⁺ cells decreased gradually in number and were seldom seen at 21 days post-injury.

At 3 days post-injury, CB2R⁺/ α -SMA⁺ cells initially appeared in the wounded site and peaked in number at 5 days after injury as detected by double indirect immunofluorescence staining (Fig. 3). With extension of posttraumatic interval, CB2R⁺/ α -SMA⁺ cells decreased gradually in number and disappeared at 21 days post-injury.

The average ratios of CB2R-positive macrophages and myofibroblasts were evaluated (Supplemental Fig. 2). The average ratios of CB2R-positive macrophages and myofibroblasts reached their climax at 3 and 5 days after injury, respectively ($P < 0.05$).

Western blotting

The blots against CB2R and GAPDH antibody are shown in Fig. 4. Western blotting analysis demonstrated that the relative ratios of CB2R to GAPDH gradually increased from 1 h post-injury onward, reached its climax at 5 days after injury, and then decreased from 7 to 21 days after injury ($P < 0.05$). Significant differences in the relative expression levels of CB2R protein were found between the control group and each posttraumatic interval from 1 h to 17 days. There were significant differences in the relative intensity of CB2R to GAPDH between 1, 5, and 10 days injury groups and their preceding groups as shown in Supplemental Fig. 3 ($P < 0.05$).

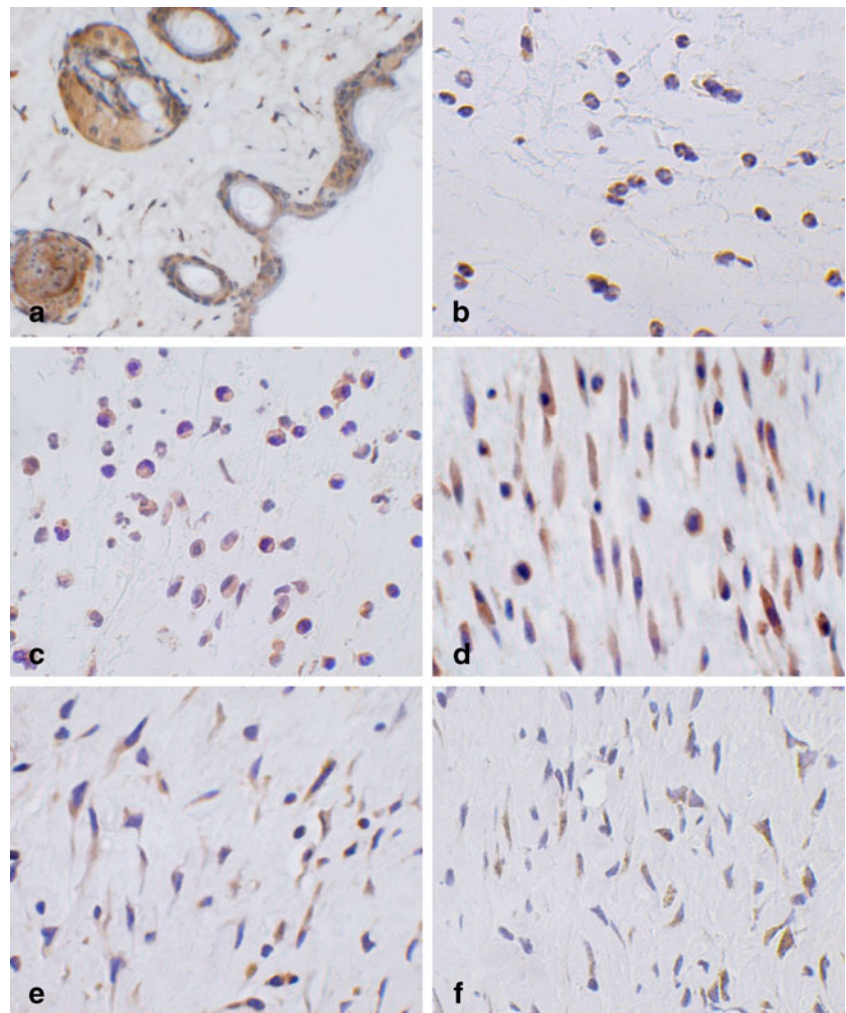
For evaluation of postmortem influence on detection of CB2R protein, it was found that no significant decrease in the relative protein level of CB2R to GAPDH was noted at 0.5, 1, 3, and 6 h as compared with that of 0 h postmortem. Continuous decrease in relative quantity of CB2R was observed from 12 h to 3 days in comparison with that of 0 h postmortem ($P < 0.05$, Fig. 5 and Supplemental Fig. 4).

Table 1 Primer sequences used for reverse transcription polymerase chain reaction

Gene	Species	Primer	Product size (bp)
CB2R	Mouse	Forward: 5'-TGGACCTGGGT GACTGG-3'	176
		Reverse: 5'-CATCTGGGATAC CTGAAACA-3'	
β -actin	Mouse	Forward: 5'-CTGTCCCTGTAT GCCTCTG-3'	217
		Reverse: 5'-TGTCACGCACGA TTTCC-3'	

Numbers (NM_) of the genes are NCBI accession numbers obtained from the NIH Database: CB2R, NM_007621; β -actin, NM_007393

Fig. 1 Immunohistochemical staining of CB2R in the control and wounded skin. **a** CB2R immunoreactivity is found in the epidermis, hair follicle, glandulae sebaceae in the uninjured control (original magnification, $\times 200$). **b, c** CB2R-positive PMNs and MNCs are detected in the wounded area at 6 h and 1 day post-wounding. **d, e** A number of spindle-shaped FBCs are positively immunostained in the wounds at 5 and 14 days after injury. **f** There were still a few FBCs labeled with CB2R antibody in the area of wound at 21 days post-injury (original magnification, $\times 400$)



Real-time PCR

The relative quantity of CB2R mRNA expression in skin specimen was assayed by real-time PCR throughout the posttraumatic intervals after incision. The relative quantity of CB2R mRNA expression was more than 4.10 at 5 days after injury, whereas less than 4.10 at the other posttraumatic intervals ($P < 0.05$). There were significant differences in the relative quantity of CB2R mRNA between 0.5 h, 1 h, 3 h, 6 h, 5 days, 7 days, 10 days, and 14 days injury groups and their preceding groups ($P < 0.05$, Supplemental Fig. 5).

In postmortem groups, no significant change was noted in CB2R mRNA levels within 3 h after death ($P > 0.05$). There was significant reduction in the CB2R mRNA levels from 6 h to 3 days compared with 0 h ($P < 0.05$, Supplemental Fig. 6).

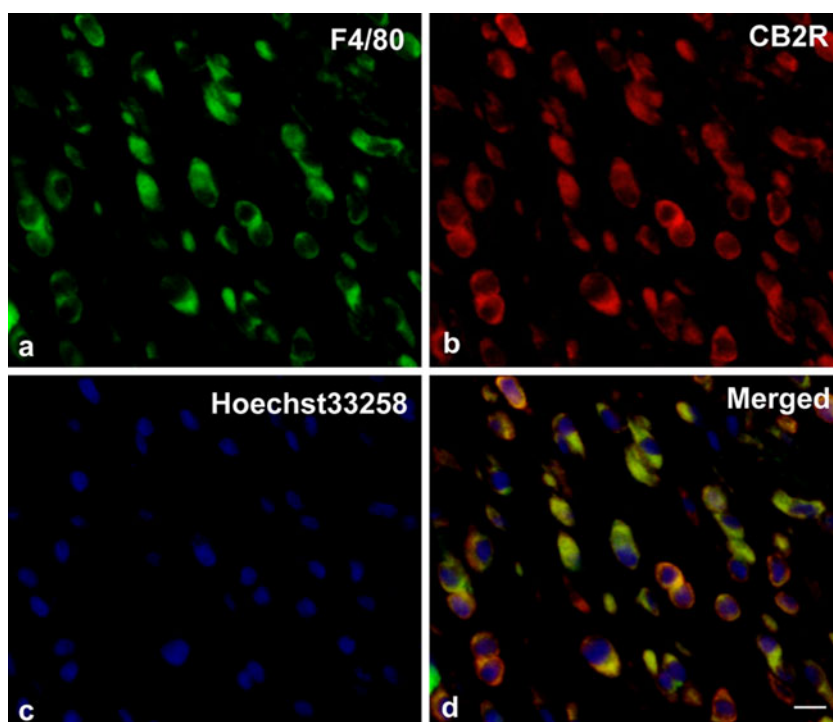
Discussion

The present study, for the first time, demonstrated that CB2R was expressed in both macrophages and myofibroblasts

infiltrated into skin wound zones during skin wound healing in mice. There is an interesting evidence that CB2R can accommodate the chemotactic response of human macrophages to chemokines CCL2-3 [16]. Peritoneal macrophage response to the chemokine RANTES/CCL5 is significantly inhibited by CB2R ligands THC and CP55,940 and by the CB2R-specific agonist O-2137. Meanwhile, the inhibition by THC is reversed by the CB2 receptor-specific antagonist SR144528. THC treatment has a minimal effect on the chemotactic response of CB2R^{-/-} peritoneal macrophages [17]. Furthermore, macrophage migration is indispensable in skin wound repair, suggesting that macrophage-derived CB2R has an effect on the modulation of macrophages in response to chemoattractants.

Myofibroblast is another CB2R-producing cell type. Betz et al. examined time-dependent appearance of α -SMA-positive myofibroblasts in human skin wounds, and demonstrated that myofibroblasts initially were detected in 5-day-old wounds and subsequently increased in number at the wound site. Besides, CB2R activation via exogenously administered cannabinoids specifically suppresses activation

Fig. 2 Double immunofluorescence analysis was performed to determine CB2R-expressing macrophages at 1 day post-injury. The samples were immunostained with anti-F4/80 (**a**, *green*) and anti-CB2R (**b**, *red*). Nuclei were counterstained with Hoechst 33258 (**c**, *blue*). Co-localization of F4/80 and CB2R is shown in the merged image (**d**, *yellow*). Representative results from five individual experiments are shown here. Scale bars=10 μ m



of pancreatic myofibroblasts. Increase in α -SMA protein levels is observed after treatment with the CB2 receptor-specific antagonist AM630 [18]. Based on these findings, we speculate that CB2R is involved in the inflammatory response of macrophages and fibrotic repair of myofibroblasts during the skin-incised wound healing.

In forensic practice, wound age estimation is one of the most important and indispensable jobs for forensic

pathologists. It is often necessary to determine wound age for correlating death with wounds. During the past 10 years, most studies on forensic wound age determination have been focused on analyses of extracellular matrix, adhesion molecules, growth factors, and cytokines [19–23]. Our data showed that immunopositive signals for CB2R were constitutively detected in the epidermis, hair follicles, sebaceous glands, cutaneous muscle layer, and vascular smooth muscle

Fig. 3 Double immunofluorescence analysis was performed to determine CB2R-expressing myofibroblasts at 5 days post-wounding. The samples were immunostained with anti- α -SMA (**a**, *green*) and anti-CB2R (**b**, *red*). Nuclei were counterstained with Hoechst 33258 (**c**, *blue*). Co-localization of α -SMA and CB2R is shown in the merged image (**d**, *yellow*). Representative results from five individual experiments are shown here. Scale bars=10 μ m

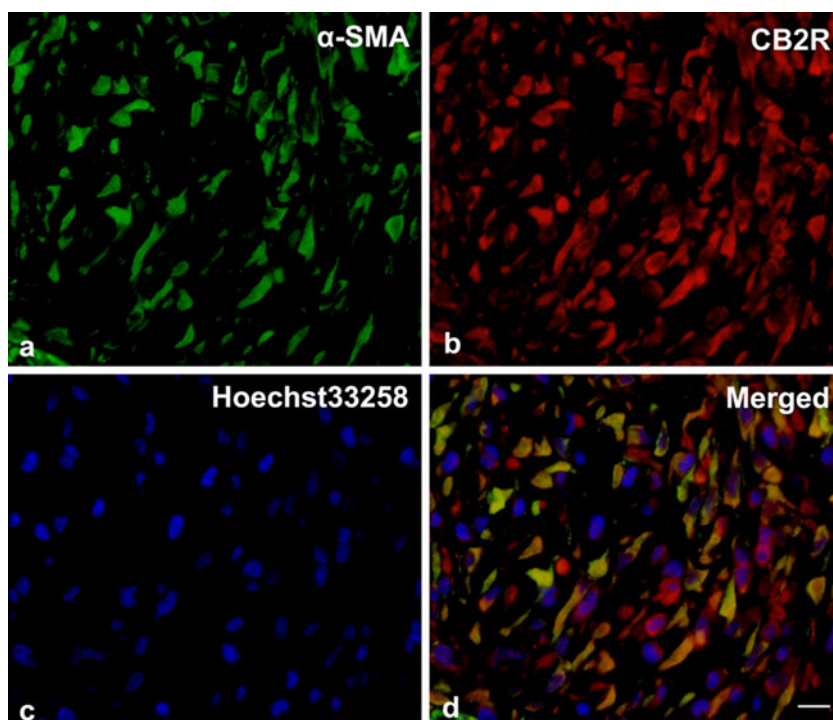
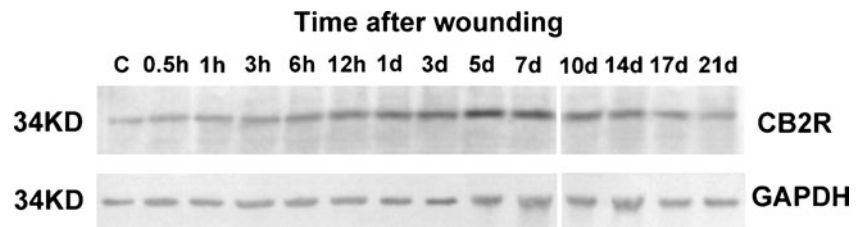


Fig. 4 Analysis of CB2R and GAPDH protein by Western blotting at different posttraumatic intervals. Lane C indicates the result of the control skin. Representative results from five individual animals are shown



cell in uninjured skin specimens. Since it was quite difficult to evaluate the difference of immunohistochemical results of the epidermis, hair follicles, sebaceous glands, and vascular smooth muscle cell between uninjured and injured skin samples, it is considered that infiltrating cells such as leukocytes and fibroblasts should be morphometrically analyzed. From the viewpoint of application of our data to forensic practice, CB2R-positive ratios of >50 % possibly indicate a wound age of 5 days as detected by immunohistochemical analysis. Moreover, positive CB2R immunoreactivity in macrophages or myofibroblasts revealed a time-dependent manner after the skin was injured. The ratio of CB2R-positive macrophages over 50 % possibly suggests a wound age of 3 days, and the ratio of CB2R-positive myofibroblasts over 65 % possibly indicates a wound age of 5 days. However, immunohistochemical staining was restricted in practical application, especially for the estimation of wound age less than 8 h, because it was not accurate and stable in a semiquantitative analysis, and the results may be influenced by investigators [24, 25]. Real-time PCR has been applied to evaluate postmortem intervals and wound age [26], which is considered to be more sensitive than immunohistochemical approaches [27] and offer the possibility to better identify the time appearance of parameters of possible future interest [28].

Recently, our research team also demonstrated that real-time PCR and Western blotting were more appropriate to detect mRNA and protein in early wound age estimation [29, 30] and suggested that CB2R would be a useful marker for wound age determination in the animal model of skeletal muscle contusion [29]. Considering the viewpoint of forensic application, the present study demonstrated that the relative ratio of CB2R mRNA expression was presumed to be a useful parameter for skin wound age determination. In real-time PCR results, the relative quantity of CB2R mRNA expression was shown to be >4.10 at 5 days post-injury.



Fig. 5 Analysis of CB2R and GAPDH protein by Western blotting at different postmortem intervals. Representative results from five individual animals are shown

After 7 days or within 5 days, no samples showed relative quantity of >4.10. Thus, the relative quantity markedly exceeding 4.10 may strongly indicate a 5-day wound age. Similarly, CB2R mRNA expression tendency was confirmed by protein expression tendency with maximized ratio of relative CB2R expression at 5 days after incision as detected by Western blotting. Based on our results, the present study demonstrated that the relative ratio of CB2R mRNA expression was presumed to be a useful parameter for skin wound age determination. Detection of CB2R by Western blotting and real-time PCR would narrow further the ranges of wound age estimation in combination with morphometrical analysis, and Western blotting and real-time PCR assays were more suitable for very early wound age estimation than immunohistochemical analysis.

It is universally accepted that degradation of mRNA and protein occurs after death, which undoubtedly interfere with application of the biological markers for estimation of wound age, although an experimental study revealed that IL-10 mRNA was detectable by RT-PCR at 5 days postmortem and might be used as a sensitive indicator of wound vitality [31]. Indeed, in forensic pathology cases, mRNA or protein is degraded gradually by means of enzymatic digestion, and different types of mRNA or proteins may have different rates of degradation. We do think that CB2R mRNA or protein would be affected by a variety of postmortem factors even if it is applicable to skin wound age determination. Based on our data, we chose wound samples at 5 days post-injury to investigate postmortem influence on the levels of CB2R protein and mRNA because expressions of CB2R protein and mRNA reached peaks at the posttraumatic time point. Compared to 0 h postmortem, no significant changes were observed in CB2R protein levels within 6 h or CB2R mRNA levels within 3 h after death under our experimental condition, suggesting that CB2R protein or mRNA might be used as a parameter for wound age estimation shortly after death.

In conclusion, CB2R is time-dependently expressed during skin wound healing in mice and might be involved in modulating macrophages and myofibroblasts in response to inflammatory event and fibrotic repair. Although further study using human samples obtained from autopsy is, of course, necessary, we propose that real-time PCR detection of CB2R could be presumed to provide significant information for wound age determination.

Acknowledgments This study was financially supported in part by a grant from research funds for the Doctoral Program funded by the Ministry of Education of China (200801590020) and a grant funded by the National Natural Science Foundation of China (30271347).

References

- Munro S, Thomas KL, Abu-Shaar M (1993) Molecular characterization of a peripheral receptor for cannabinoids. *Nature* 365:61–65
- Kishimoto S, Muramatsu M, Gokoh M, Oka S, Waku K, Sugiura T (2005) Endogenous cannabinoid receptor ligand induces the migration of human natural killer cells. *J Biochem* 137:217–223
- Oka S, Ikeda S, Kishimoto S, Gokoh M, Yanagimoto S, Waku K, Sugiura T (2004) 2-arachidonoylglycerol, an endogenous cannabinoid receptor ligand, induces the migration of EoL-1 human eosinophilic leukemia cells and human peripheral blood eosinophils. *J Leukoc Biol* 76:1002–1009
- Facci L, Dal Toso R, Romanello S, Buriani A, Skaper SD, Leon A (1995) Mast cells express a peripheral cannabinoid receptor with differential sensitivity to anandamide and palmitoylethanolamide. *Proc Natl Acad Sci U S A* 92:3376–3380
- Matias I, Pochard P, Orlando P, Salzet M, Pestel J, Di Marzo V (2002) Presence and regulation of the endocannabinoid system in human dendritic cells. *Eur J Biochem* 269:3771–3778
- Galiègue S, Mary S, Marchand J, Dussosoy D, Carrière D, Carayon P, Bouaboula M, Shire D, Le Fur G, Casellas P (1995) Expression of central and peripheral cannabinoid receptors in human immune tissues and leukocyte subpopulations. *Eur J Biochem* 232:54–61
- Mackie K (2006) Cannabinoid receptors as therapeutic targets. *Annu Rev Pharmacol Toxicol* 46:101–122
- Buckley NE (2008) The peripheral cannabinoid receptor knockout mice: an update. *Br J Pharmacol* 153:309–318
- Brown AJ (2007) Novel cannabinoid receptors. *Br J Pharmacol* 152:567–575
- Ständer S, Schmelz M, Metze D, Luger T, Rukwied R (2005) Distribution of cannabinoid receptor 1 (CB1) and 2 (CB2) on sensory nerve fibers and adnexal structures in human skin. *J Dermatol Sci* 38:177–188
- Karsak M, Gaffal E, Date R, Wang-Eckhardt L, Rehnelt J, Petrosino S, Starowicz K, Steuder R, Schlicker E, Cravatt B, Mechoulam R, Buettner R, Werner S, Di Marzo V, Tüting T, Zimmer A (2007) Attenuation of allergic contact dermatitis through the endocannabinoid system. *Science* 316:1494–1497
- Oka S, Wakui J, Ikeda S, Yanagimoto S, Kishimoto S, Gokoh M, Nasui M, Sugiura T (2006) Involvement of the cannabinoid CB2 receptor and its endogenous ligand 2-arachidonoylglycerol in oxazolone-induced contact dermatitis in mice. *J Immunol* 177:8796–8805
- Ueda Y, Miyagawa N, Matsui T, Kaya T, Iwamura H (2005) Involvement of cannabinoid CB(2) receptor-mediated response and efficacy of cannabinoid CB(2) receptor inverse agonist, JTE-907, in cutaneous inflammation in mice. *Eur J Pharmacol* 520:164–171
- Akhmetshina A, Dees C, Busch N, Beer J, Sarter K, Zwerina J, Zimmer A, Distler O, Schett G, Distler JH (2009) The cannabinoid receptor CB2 exerts antifibrotic effects in experimental dermal fibrosis. *Arthritis Rheum* 60:1129–1136
- Kondo T, Ohshima T (1996) The dynamics of inflammatory cytokines in the healing process of mouse skin wound: a preliminary study for possible wound age determination. *Int J Legal Med* 108:231–267
- Montecucco F, Burger F, Mach F, Steffens S (2008) CB2 cannabinoid receptor agonist JWH-015 modulates human monocyte migration through defined intracellular signaling pathways. *Am J Physiol Heart Circ Physiol* 294:H1145–H1155
- Raborn ES, Marciano-Cabral F, Buckley NE, Martin BR, Cabral GA (2008) The cannabinoid delta-9-tetrahydrocannabinol mediates inhibition of macrophage chemotaxis to RANTES/CCL5: linkage to the CB2 receptor. *J Neuroimmune Pharmacol* 3:117–129
- Michalski CW, Maier M, Erkan M, Sauliunaite D, Bergmann F, Pacher P, Batkai S, Giese NA, Giese T, Friess H, Kleeff J (2008) Cannabinoids reduce markers of inflammation and fibrosis in pancreatic stellate cells. *PLoS One* 3:e1701
- Ortiz-Rey JA, Suárez-Peñaranda JM, Da Silva EA, Muñoz JI, San Miguel-Fraile P, De la Fuente-Buceta A, Concheiro-Carro L (2002) Immunohistochemical detection of fibronectin and tenascin in incised human skin injuries. *Forensic Sci Int* 126:118–122
- Liu N, Chen Y, Huang X (2006) Fibronectin EIIIA splicing variant: a useful contribution to forensic wounding interval estimation. *Forensic Sci Int* 162:178–182
- Dressler J, Bachmann L, Strejc P, Koch R, Müller E (2000) Expression of adhesion molecules in skin wounds: diagnostic value in legal medicine. *Forensic Sci Int* 113:173–176
- Grellner W, Vieler S, Madea B (2005) Transforming growth factors (TGF-alpha and TGF-beta1) in the determination of vitality and wound age: immunohistochemical study on human skin wounds. *Forensic Sci Int* 153:174–180
- Grellner W (2002) Time-dependent immunohistochemical detection of proinflammatory cytokines (IL-1beta, IL-6, TNF-alpha) in human skin wounds. *Forensic Sci Int* 130:90–96
- Takamiya M, Saigusa K, Kumagai R, Nakayashiki N, Aoki Y (2005) Studies on mRNA expression of tissue-type plasminogen activator in bruises for wound age estimation. *Int J Legal Med* 119:16–21
- Bai R, Wan L, Shi M (2008) The time-dependent expressions of IL-1beta, COX-2, MCP-1 mRNA in skin wounds of rabbits. *Forensic Sci Int* 175:193–197
- Bauer M (2007) RNA in forensic science. *Forensic Sci Int Genet* 1:69–74
- Kondo T, Ishida Y (2010) Molecular pathology of wound healing. *Forensic Sci Int* 203:93–98
- Cecchi R (2010) Estimating wound age: looking into the future. *Int J Legal Med* 124:523–536
- Yu TS, Cheng ZH, Li LQ, Zhao R, Fan YY, Du Y, Ma WX, Guan DW (2010) The cannabinoid receptor type 2 is time-dependently expressed during skeletal muscle wound healing in rats. *Int J Legal Med* 124:397–404
- Ma WX, Yu TS, Fan YY, Zhang ST, Ren P, Wang SB, Zhao R, Pi JB, Guan DW (2011) Time-dependent expression and distribution of monoacylglycerol lipase during the skin-incised wound healing in mice. *Int J Legal Med* 125:549–558
- Ohshima T, Sato Y (1998) Time-dependent expression of interleukin-10 (IL-10) mRNA during the early phase of skin wound healing as a possible indicator of wound vitality. *Int J Legal Med* 111:251–255